Journal of the Mechanics and Physics of Solids 61 (2013) 1265–1279

Contents lists available at SciVerse ScienceDirect

Journal of the Mechanics and Physics of Solids

journal homepage: www.elsevier.com/locate/jmps

Peeling of a tape with large deformations and frictional sliding

Matthew R. Begley [a,b,*], Rachel R. Collino [a], Jacob N. Israelachvili [b,c], Robert M. McMeeking [a,b,d,e]

[a] Department of Mechanical Engineering, University of California, Santa Barbara, CA 93106, USA
[b] Materials Department, University of California, Santa Barbara, CA 93106, USA
[c] Department of Chemical Engineering, University of California, Santa Barbara, CA 93106, USA
[d] School of Engineering, University of Aberdeen, King's College, Aberdeen AB24 3UE, Scotland, UK
[e] INM - Leibniz Institute for New Materials, Campus D22, 66123, Saarbrücken, Germany

ARTICLE INFO

Article history:
Received 31 January 2012
Received in revised form
6 September 2012
Accepted 21 September 2012
Available online 8 October 2012

Keywords:
Peel test
Slip
Large deformation
Thin film adhesion

ABSTRACT

An analytical model of peeling of an elastic tape from a substrate is presented for large deformations and scenarios where sliding occurs in the adhered regions, with this motion resisted by interfacial shear tractions. Two geometries are considered: the first has a detached segment of the tape forming the shape of an inverted letter 'V' between adhered sections (double-sided peeling), and the second has a free end of the tape being pulled (single-sided peeling). The mechanics of peeling is analyzed in terms of the applied force, displacement of the load point and the angle that the peeled tape makes with the substrate. Formulae are provided for the energy released per unit area of peeling that explicitly and separately account for the work done by frictional sliding. Assuming that peeling occurs when the energy released per unit area equals the work of separation for purely normal separation, it is shown that the critical force to propagate peeling can be significantly higher with sliding as compared to pure sticking. Similarly, due to frictional dissipation, the amount of work done by the applied force needed to propagate peeling can be significantly greater than the work of separation. For the single-sided peel test, an effective mixed-mode interface toughness is presented to be used with purely sticking models when sliding is not explicitly modeled: the closed-form result closely mirrors common empirical forms used to predict mixed-mode delamination.

1. Introduction

The detachment of a tape from a substrate by peeling it away is an important technological process that relates to adhesion and the use of adhesive tape to fix objects in place. In addition, it can serve as a model for more complicated phenomena such as the ability of plants and animals (notably geckos and mussels, e.g., Pesika et al., 2007; Cheng et al., 2012; Sauer, 2011) to cling to a surface, resisting gravity, aerodynamic or fluidic drag, predatory efforts to remove them, etc. In many biological and synthetic systems, the interfacial bond between surfaces need not be strongly chemical (with cross-linking or the insertion of functional groups into adjacent surfaces), but can be physical such as occurs in van der Waals adhesion or electrostatics.

Such physical bonds are often referred to as "weak", due to the relatively small energy that is required to break them in comparison to covalent bonds. However, the term "weak bonding" does not translate into "weak adhesion", since such bonds are

* Corresponding author. Tel.: +1 805 679 1122.
E-mail address: begley@engr.ucsb.edu (.

0022-5096/$ - see front matter © 2012 Elsevier Ltd. All rights reserved.
http://dx.doi.org/10.1016/j.jmps.2012.09.014

routinely exploited in adhesive systems that require extremely large forces and/or remotely applied work to drive debonding. This highlights the necessity and importance of distinguishing between the locally defined energy required to break bonds at the interface, and other measures of the work required to drive debonding. Rather large differences between such quantities arise when there are dissipative mechanisms that are triggered by the application of remote loads. This has been clearly demonstrated for various tape systems that utilize thin, viscoelastic adhesive layers between the tape and the substrate: e.g., Newby et al. (1995), Newby and Chaudhury (1997, 1998), and Amouroux et al. (2001).

In this work, we address the problem of peeling an elastic tape from a rigid substrate, where frictional sliding occurs at the interface: the overarching goal is to quantify the role of friction in altering the applied forces and displacements required to propagate peeling. Two different geometries are analyzed, as shown in Fig. 1 (double-sided 'V'-peeling) and Fig. 2 (single-sided peeling). In both geometries, there is an initial tape segment that does not adhere to the substrate: this segment is defined by its

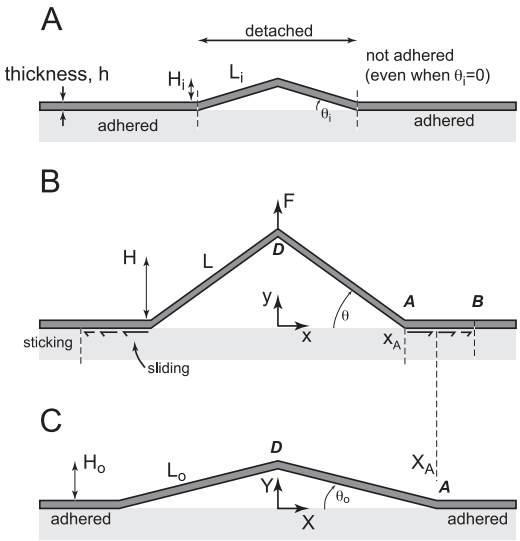

Fig. 1. Schematic of the double-sided "V" peel test and variables used in the analysis; (A) the initial configuration defines the position of the tape prior to any peeling, with no tension in the tape anywhere, (B) the deformed position after load is applied, with peeling, sliding and stretching having taken place, and (C) the peeled configuration in which the tape is free of tension (used as a reference in the analysis). The edge of attachment is given as point *A*, with x_A indicating the position of the edge in the loaded (deformed configuration), and X_A indicating the position of the same point in the unloaded (but peeled) configuration. Beyond point *B*, the tape remains adhered (stuck) with no deformation. A vertical force is applied to point *D*.

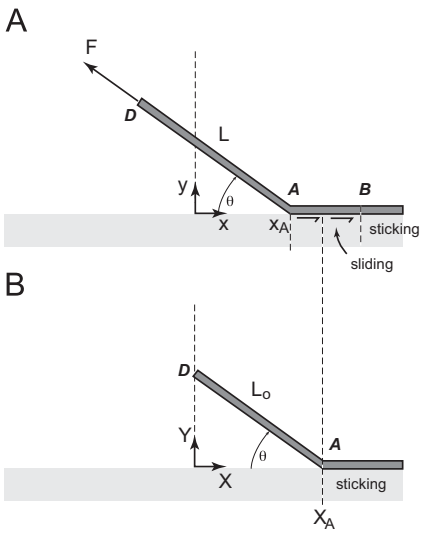

Fig. 2. Schematic of the single-sided peel test and variables used in the analysis; (A) the deformed position after load is applied, with peeling, sliding and stretching having taken place and (B) the unloaded configuration in which the tape is free of tension (used as a reference in the analysis). The edge of attachment is given as point *A*, with x_A indicating the position of the edge in the loaded (deformed configuration), and X_A indicating the position of the same point in the unloaded configuration. Beyond point *B*, the tape remains adhered (stuck) with no deformation. A tangential force is applied to point *D*.

length, L_i, and the initial angle in the unloaded state. Even when the tape is initially lying flat prior to the application of load (i.e., $\theta_i = 0$), there is no attractive force in the segment defined by L_i. The case of pulling a perfectly flat tape that is completely adhered requires explicit treatment of the cohesive force–displacement relationship and is not considered here.

The analysis predicts the relationship between the applied force, the initial (unloaded) configuration, and the deformed geometry, subject to the condition that the change in system energy with an increment in detached length is equal to the work of normal separation: i.e., the energy required to separate two surfaces via purely normal displacements. We consider very thin tapes such that the bending stiffness is negligible and present a large deformation analysis that accounts for significant changes in tape orientation and can account for elastically non-linear material response. Upon application of remote loading, the tape experiences stretching, peeling, and sliding near the edge of contact. As the applied force is increased, the length of peeled (detached) tape increases and the edge of the sliding zone (point B in Figs. 1 and 2) propagates outwards. As will be shown, the applied force required to propagate peeling will reach a steady-state in 'V'-peeling when the peeled length of the tape greatly exceeds the initial length, in that the applied force asymptotes to a constant value. In the limit of steady-state peeling, neither the applied force required to drive peeling nor the deformed angle of the tape (under load) changes: we show that the deformed geometry evolves in a self-similar fashion.

While the present analysis does not consider the case where the sliding zone reaches the end of the tape, the applied force required to propagate peeling is expected to decrease after this point, since frictional forces will decrease with the length of the sliding zone. Hence, the steady-state force required to propagate peeling is equivalent to the detachment force for the entire tape, also commonly referred to as the adhesion force. Naturally, short tapes might not be long enough to reach steady-state, and the adhesion force (i.e., the applied force needed to completely remove the tape) will be smaller than that predicted here. In that regard, the steady-state limit of the present analysis represents an upper bound on the force required to completely remove the tape.

It should be emphasized at the outset that the case of single-sided peeling in our analysis is by definition in the steady-state limit, because the force is applied at a constant angle relative to the substrate even as peeling propagates. This is because a tape (represented as a membrane with no bending stiffness) must be aligned with the applied force direction. While our assumption of a constant loading angle enforces a somewhat artificial displacement trajectory to the load point, other scenarios can be analyzed using the results presented here.

By explicitly modeling sliding displacements near the edge of detachment, the framework developed here explicitly accounts for the work dissipated by sliding. The present model reduces in the limit of no sliding and small deformation to the seminal results by Kendall (1971, 1975) for single-sided peeling, and for double-sided peeling to that of Gent and Kaang (1986) and several others (e.g., Williams, 1997; Wan, 1999; Sun et al., 2004). In the limit of zero sliding displacements but large deformation, the present single-sided peeling model is ostensibly the same as the large-deformation 'sticking' analysis of Molinari and Ravichandran (2008).

To our knowledge, there have been only a few treatments of elastic tape adhesion in which sliding displacements have been explicitly addressed. Notable is the work of Newby et al. (1995); Newby and Chaudhury (1997, 1998), in which peel tests were conducted for a poly-(dimethylsiloxane) (PDMS) tape on a substrate functionalized with PDMS polymer chains. Their analysis explicitly calculates the rate-dependent shear stress in the viscoelastic layer at the interface using experimental slip displacements at the edge of peeling. From the shear stress they calculate the amount of frictional energy that is dissipated: it is shown that frictional sliding dissipates significant energy in comparison to the work of adhesion for purely normal separation. Their approach differs from the present work in that the experimental energy released by peeling is computed from peel forces using Kendall's result for pure sticking: frictional sliding is accounted for by adding the frictional energy dissipated (calculated from slip displacements) to the work of adhesion for purely normal separation. Here, our peeling criterion does not depend on frictional sliding: frictional sliding influences the force required to propagate peeling, but not the energy balance associated with the onset of peeling. Additional work is needed to examine the commonality between these two approaches, and explore the possible roles of additional dissipation mechanisms (as noted in Newby and Chaudhury, 1997), as well as the possibility that critical sliding displacements exist at which polymer chains across the interface detach and alter the sliding stress. The present theoretical results for slip-independent interfacial shear stress do not consider this possibility, although such behavior can be deduced from the general analysis presented here.

In a previous treatment of frictional sliding, Chen et al. analyzed peeling using cohesive elements that allowed for frictional sliding (Cheng et al., 2012; Chen et al., 2009). In their work, the cohesive tractions are a function of both sliding and opening displacements, and frictional sliding is permitted in the adhered region that has zero opening. It is demonstrated that allowing sliding displacements prior to peeling (which result in tape "pre-tension" in the adhered tape) increases the pull-off force for a given peel angle. As will be discussed, their numerical simulations show behavior that is consistent with the analytical results presented here.

The work presented here is analogous in some respects to that of Wang and Li (2007), who analyze the problem of a linear-elastic tape that is pinned at its outer boundaries, and adhered to a flat punch that is pulled upwards. Frictionless sliding is permitted in the adhered region on the punch. Interestingly, in this case, they show that sliding reduces the apparent work of adhesion: sliding permits an increase in the angle of the tape running from the punch to the substrate, which increases the normal forces driving separation. Though similar to the geometry in Fig. 1, direct comparisons to this work are not appropriate, since peeling and sliding occurs at the load point (where the punch is attached) rather than on the substrate.

Finally, the present analysis of frictional sliding is analogous in some respects to a large body of work that considers the effects of bending and/or bulk dissipation (either in the film or in a ductile adhesive layer), but does not explicitly address

the influence of interface sliding. For examples, see Sauer (2011), Tsai and Kim (1993), Tvergaard and Hutchinson (1993), Kinloch et al. (1994), Wei and Hutchinson (1998), Lu et al. (2007), Thouless and Yang (2008), Sun and Dillard (2010), Plaut and Ritchie (2004) and references therein. Many of these studies adopt a mixed-mode fracture criterion, wherein the conditions controlling debonding depend on the relative tangential displacements between the substrate and film. This can be done either with a cohesive law involving interfacial shear stress or an effective interface toughness that depends on the relative amounts of normal and shear stress across the interface. The models differ from the present study because debonding can be triggered purely by interfacial shear stresses (e.g., debonding occurs when sliding displacements in the cohesive law reach a critical value). In the limit of "brittle" interfaces (or small plastic zones), these models reduce to Kendall-type predictions which correspond to pure sticking (Kendall, 1971, 1975). Connection is made to these approaches in Section 5.2, which discusses equivalent mixed-mode fracture criteria that bring the sliding model into coincidence with sticking models.

2. Overview of the model

2.1. Description of the process of peeling with sliding

Consider the tape stuck to a rigid substrate in the configuration shown in Fig. 1. There is a central segment that is initially detached, and the detached regions form an inverted "V". The configuration shown in Fig. 1A refers to the initial, unstressed configuration of the tape as it is laid on the substrate, prior to the application of any force or any peeling. The length of the detached tape segments is L_i and they form the angle θ_i when the tape is placed on the substrate and the arms of the "V" are straight. When the initial angle is zero, the tape is placed flat with a central region of length $2L_i$ that does not adhere to the substrate. Again, the case of a completely adhered flat tape requires explicit inclusion of the force–displacement relationship describing cohesion and molecular contact, and is not considered here.

After force is applied to the tip of the "V", the length of the detached tape increases due to (i) peeling, (ii) stretching, and (iii) sliding of the adhered tape near the edge of attachment. The direction of sliding under increasing load is inwards, towards the origin. In the deformed state shown in Fig. 1B, the length of the detached region is L, while the angle formed with the substrate is θ. The angle of the tape in the deformed state can be either larger than its initial configuration (e.g., due to inward sliding without peeling) or smaller (e.g., due to peeling with comparatively small sliding). It is assumed that the sliding region at the edge of the tape is smaller than the distance to the end of the tape, such that there is always a portion of tape that remains undeformed.

An increment in peeling is defined here as an increment in the *undeformed* length of the detached tape. After peeling has propagated some distance, the undeformed length of the detached tape is no longer L_i. Fig. 1C depicts the *undeformed* state of the tape after peeling has propagated: L_0 is the length of the undeformed detached tape segment, while θ_0 is the angle the undeformed detached segment forms with the substrate. In the analysis of sliding that follows, we preclude the possibility of unloading, as it could lead to a reversal in the sliding direction at the edge of attachment. Thus, the unstressed and peeled configuration in Fig. 1C is merely used as a reference: we utilize the unstressed peeled length L_0 as an implicit parameter to describe the extent of peeling, with the understanding that only the initial configuration and the deformed states are observable via experiment without violating the sliding assumption in the model. We refer to the case with $L_0 = L_i$ as peeling initiation, while scenarios with $L_0 > L_i$ are termed peeling propagation. As will be shown, when $L_0 \gg L_i$ (i.e., significant peeling has occurred), the force required to propagate peeling asymptotes to a constant value, as does the deformed angle θ: this is referred to here as steady-state peeling.

For single-sided peeling, the process is identical: tension applied to the tape leads to tape stretching, sliding at the edge of attachment, and peeling. Since the tape must remain aligned with the direction of loading (due to the membrane approximation), the initial, deformed and reference configurations are characterized by the same angle $\theta_i = \theta_0 = \theta$. Again, this is a consequence of the assumption that the load is applied at a fixed angle to the substrate: other loading paths (where the direction of the applied force changes as it is increased) can be easily constructed from the results presented here. The analysis of single-sided peeling is presented as a straightforward simplification of the double-sided case.

In the present analyses, peeling is controlled by the condition that the energy released by peeling is equal to the work of separation (adhesion) for the interface, $G = \Gamma_i$, where Γ_i is explicitly defined as the work of adhesion for purely normal separation. The energy released by peeling is computed by considering the incremental changes in work/energy that arise due to an incremental change in the unstressed peeled length of tape, dL_0 (see Fig. 1). The increment dL_0 leads to incremental changes in the deformed state of the tape, which cause incremental changes in strain energy (in both the detached and sliding regions), incremental work done by the applied force, and incremental work done by the sliding displacements. These are analyzed below to establish the critical forces and displacements required to cause peeling, given Γ_i. Section 5 provides a detailed discussion of the roles of sliding work versus work of separation, and how these physical phenomena factor into predictions of peeling.

2.2. Material response and sliding behavior

Let the tape material be elastic but capable of large strain. Such an assumption enables analysis of the problem at any level of strain and with arbitrary changes to the geometry; the results can be specialized to the limiting case of

infinitesimal strain thereafter. The tape free energy per unit volume, ψ, is such that

$$T_i = \frac{\partial \psi}{\partial \lambda_i} \tag{1}$$

where T_i are the principal nominal (1st Piola-Kirchhoff) stress components and λ_i are the principal stretch ratios. Let the stretch ratio parallel to the lengthwise direction of the tape be λ, and T is the component of the stress in the same direction. We consider T to be the average value through the thickness of the tape, and λ to be effectively the average value as well, though some asymptotic approximation is involved in this assumption. The force in the tape at a given position (parallel to the orientation of the tape at that position) is given by

$$P = wh\frac{\partial \psi}{\partial \lambda} \tag{2}$$

where w is the width of the tape. Thus, if the stretch ratio is known at a given location, then we know the related tape tensions. As a consequence, we can write the relationship between the deformed and undeformed location of the edge of detachment as

$$x_A(X_A, \lambda_A) = X_A - f(\lambda_A) \tag{3}$$

where f is a function that must be computed from the mechanics solution of the sliding tape, and λ_A is the axial stretch ratio at the edge of detachment. Effectively, $f(\lambda_A)$ represents the negative of the displacement of the tape at point A. Note that there are restrictions on the nature of the frictional shear drag that must be met before Eq. (3) is valid. Suffice it to say that a uniform frictional shear stress τ is satisfactory for Eq. (3) to be valid, so we are at least able to handle that case, as described in Section 5.3.

3. Double-sided peeling

3.1. General analysis

Consider the deformed geometry shown in Fig. 1B and the reference geometry shown in Fig. 1C. As described in Section 2.1, an increment in peeling is defined as an incremental change in the unstressed length of the film, dL_0. Since an initially flat segment is peeled, the change in the undeformed length associated with the increment in peeling is given by $dL_0 = dX_A$. This incremental peeling event (i.e., a change in the unstressed length of detached tape) causes incremental changes in the deformed configuration, i.e., dL and $d\theta$, and the stretch in the tape $d\lambda$. These changes lead to incremental changes in strain energy both in the detached segment and the sliding segment, as well as increments in work done at the load-point (D) and the edge of the sliding region (A). We now proceed to calculate the incremental changes in strain energy and work associated with the peeling increment dL_0.

The incremental work done by the applied force at point D due to the peeling increment dL_0 can be written as $dW_F = F \cdot dy_D$, where dy_D is the incremental change in vertical position of D that results from the peeling increment. The length of the detached segment in the deformed geometry is given by $L = \lambda_D L_0$, where λ_D is the axial stretch ratio in the detached segment of tape. The change in height of point D due to the peeling event is given by

$$dy_D = d(\lambda_D L_0 \sin\theta) = (\lambda_D\, dL_0 + L_0\, d\lambda_D)\sin\theta + \lambda_D L_0 \cos\theta\, d\theta \tag{4}$$

where $d\lambda_D$ and $d\theta$ are the incremental changes in the tape stretch and orientation due to the change in state. The change in the x-position of point D due to the peeling increment is constrained to be zero. The change in x_D can be written as the change in the position of point A due to peeling minus the change in position due to the change in tape length:

$$dx_D = dx_A - d(\lambda_D L_0 \cos\theta) = 0 = dL_0 - \frac{df}{d\lambda}d\lambda_A - (\lambda_D\, dL_0 + L_0\, d\lambda_D)\cos\theta + \lambda_D L_0 \sin\theta\, d\theta = 0 \tag{5}$$

where it has been noted that $dX_A = dL_0$. We then eliminate the increment of rotation $d\theta$ from Eqs. (4) and (5) to obtain

$$dy_D = \frac{1}{\sin\theta}(\lambda_D\, dL_0 + L_0\, d\lambda_D) - \frac{dL_0}{\tan\theta} + \frac{1}{\tan\theta}\frac{df(\lambda_A)}{d\lambda}\, d\lambda_A \tag{6}$$

From equilibrium in the deformed configuration, we can deduce that the tension in the detached tape is given by

$$\frac{F}{2\sin\theta} = wh\frac{\partial \psi(\lambda_D)}{\partial \lambda} \tag{7}$$

and that the force at the point A in the attached tape is

$$\frac{F}{2\tan\theta} = wh\frac{\partial \psi(\lambda_A)}{\partial \lambda} \tag{8}$$

The expression for the work done by the applied load is therefore:

$$dW_F = \frac{F}{\sin\theta}(\lambda_D\, dL_0 + L_0\, d\lambda_D) + \frac{F}{\tan\theta}\left[\frac{df(\lambda_A)}{d\lambda}d\lambda_A - dL_0\right] \tag{9}$$

The work done at the boundary between detached tape and adhered tape, as this point slides due to the peeling increment, is given by

$$dW_A = -\frac{F}{2\tan\theta} du_A \tag{10}$$

where du_A is the incremental change in displacement of the *far* end of the segment dL_0 associated with the peeling event. In the deformed state and prior to peeling, the deformed position of the right end of the segment to be peeled is at $x(X_A+dL_0,\lambda_A) = x_A(X_A,\lambda_A)+\lambda_A\, dL_0$, a consequence of the fact that the segment dL_0 is deformed prior to peeling. Prior to peeling, the position of the point that will form the new edge of detachment is given by

$$x(X_A+dL_0,\lambda_A) = x_A(X_A,\lambda_A)+\lambda_A\, dL_0 = \left[X_A - f(\lambda_A)\right]+\lambda_A\, dL_0 \tag{11}$$

where the second equation is obtained by noting that $x_A = X_A - f(\lambda_A)$, by definition.

We now require the conditions *after* peeling by dL_0 to be such that the stretch ratio at the new end of the attached tape becomes $\lambda_A+d\lambda_A$ and the stretch ratio in the detached segment becomes $\lambda_D+d\lambda_D$. This requirement allows for any reconfiguration that might be associated with the peeling increment, e.g., an increase in the adhesion energy along the substrate that causes the force required to propagate peeling to increase as the detachment process takes place. However, we will avoid situations in which the sliding direction reverses so that frictional drag will always act in the same direction.

As a consequence of peeling, the position in the deformed configuration at the end of the still attached portion of the tape, after peeling will be

$$x_A+dx_A = (X_A+dX_A)-(f+df) = X_A+dL_0-\left(f(\lambda_A)+\frac{df}{d\lambda_A}d\lambda_A\right) \tag{12}$$

The displacement of the edge of detachment during the peeling event is given by the difference of Eq. (12) and Eq. (11); i.e., it is the difference between the deformed configuration of the point lying at the undeformed coordinate X_A+dL_0 prior to peeling, and the final deformed position of the edge of attachment after peeling. Subtracting Eq. (11) from (12) yields

$$du_A = -\frac{df}{d\lambda_A}d\lambda_A-(\lambda_A-1)\, dL_0 \tag{13}$$

With this result, the work done at the boundary between the detached and adhered tape is given by

$$dW_A = \frac{F}{2\tan\theta}\left(\frac{df}{d\lambda_A}d\lambda_A+(\lambda_A-1)\, dL_0\right) \tag{14}$$

The change in strain energy in the detached segment of tape is given by

$$dU_D = d(wh\psi(\lambda_D)L_0) = wh\psi(\lambda_D)\, dL_0+whL_0\frac{\partial\psi}{\partial\lambda_D}d\lambda_D = wh\psi(\lambda_D)\, dL_0+\frac{FL_0 d\lambda_D}{2\sin\theta} \tag{15}$$

where the derivative of the strain energy is replaced with the applied force using Eq. (7). The strain energy, $wh\psi(\lambda_A)$ in each of the two segments $dX_A = dL_0$ that are now detached is also released during the peeling event.

Considering all energy/work changes, the equation that gives the energy released during peeling is given by

$$2G\cdot w\cdot dL_0 = dW_F-2dW_A-2dU_D+2wh\psi(\lambda_A)dL_0 \tag{16}$$

where we have recognized that, due to symmetry, an area of the tape equal to $2wdL_0$ is detached due to peeling as well as the fact that there are two attachment points and two legs. Combining all terms, the result is

$$\begin{aligned} 2G\cdot w\cdot dL_0 = {} & \frac{F}{\sin\theta}(\lambda_D\, dL_0+L_0\, d\lambda_D)+\frac{F}{\tan\theta}\left[\frac{df(\lambda_A)}{d\lambda}d\lambda_A-dL_0\right]-2wh\psi(\lambda_D)\, dL_0-\frac{F}{\sin\theta}L_0\, d\lambda_D+2wh\psi(\lambda_A)\, dL_0 \\ & -\frac{F}{\tan\theta}\left[\frac{df(\lambda_A)}{d\lambda}\, d\lambda_A+(\lambda_A-1)\, dL_0\right] \end{aligned} \tag{17}$$

which simplifies to

$$G = \frac{F}{2w}\left(\frac{\lambda_D}{\sin\theta}-\frac{\lambda_A}{\tan\theta}\right)+h[\psi(\lambda_A)-\psi(\lambda_D)] \tag{18}$$

This expression is a universal result valid for the peeling of any elastic material, as long as the frictional drag is consistent with our assumptions. For example, it is valid for a uniform sliding stress and for a tape that does not slide at all (i.e., pure sticking). For pure sticking, $\lambda_A = 1$ and $\psi(\lambda_A) = 0$, and we recover the results derived earlier for 'V'-peeling (Gent and Kaang, 1986; Williams, 1997; Wan, 1999).

It is somewhat surprising to note that the frictional sliding stress τ does not appear in the final expression for critical force when sliding occurs. This is because the frictional work term is exactly balanced by an increase in work done by the applied load. Friction will be shown to impact the load–displacement curve resulting from a peel test, and the relationship between the initial (unstressed angle) and the deformed angle at the instance of peeling. It does not, however, impact the relationship between the critical force for peeling propagation associated with the deformed angle.

3.2. Energy released by peeling for small strains: double-sided peeling

For infinitesimal straining, the stretch ratio in the tape is related to strain via $\lambda = 1+\epsilon$, where ϵ is the axial strain in the tape. We have

$$\epsilon_D = \frac{F}{2Ehw\sin\theta}, \quad \epsilon_A = \frac{F}{2Ewh\tan\theta}, \quad \psi(\lambda_D) = \frac{E}{2}\left(\frac{F}{2Ewh\sin\theta}\right)^2, \quad \psi(\lambda_A) = \frac{E}{2}\left(\frac{F}{2Ewh\tan\theta}\right)^2 \tag{19}$$

where E is the Young's modulus of the tape. To simplify the notation, we define a dimensionless force as $\overline{F} = F/(Ewh)$: note that the small strain assumption implies that $\overline{F} \ll 1$. The corresponding normalized energy released by the peeling process is $\overline{G} = G/(Eh)$. Using these definitions with Eq. (18), the energy released by the peeling process for 'V'-peeling is

$$\overline{G} = \frac{1}{2}\overline{F}\tan\frac{\theta}{2} + \frac{1}{8}\overline{F}^2 \tag{20}$$

This can be solved to calculate the critical force for peeling propagation by setting $\overline{G} = \overline{\Gamma}_i$, where $\overline{\Gamma}_i = \Gamma_i/Eh$ is the normalized work of adhesion of the interface: the relevant root is given by

$$\overline{F}_c = \sqrt{8\overline{\Gamma}_i + 4\tan^2\frac{\theta}{2}} - 2\tan\frac{\theta}{2} \tag{21}$$

Note that the above results represent the conditions for peeling propagation regardless of whether or not steady-state has been reached. (As is demonstrated in Section 5.3 for 'V'-peeling, the deformed peeling angle θ and load $\overline{F}$ evolve with applied displacement as a tape is peeled, but asymptote to constant values.) Also, Eqs. (19–21) are no longer universal, as they do not apply for pure sticking scenarios. For pure sticking, $\lambda_A = 1$ and $\psi(\lambda_A) = 0$. One obtains the following (Gent and Kaang, 1986; Williams, 1997; Wan, 1999):

$$\overline{G}^{stick} = \frac{1}{2}\overline{F}\tan\frac{\theta}{2} + \frac{1}{8}\left(\frac{\overline{F}}{\sin\theta}\right)^2 \tag{22}$$

$$\overline{F}^{stick} = 2\sqrt{\overline{\Gamma}(1-\cos 2\theta) + 4\sin^4\frac{\theta}{2}\sin^2\theta} + \sin 2\theta - 2\sin\theta \tag{23}$$

Fig. 3A shows the predictions for peeling with sliding and peeling without sliding assuming infinitesimal strains, which are very different for peel angles less than 20°. For pure sticking, the peeling force asymptotes to zero at small peel angles, while for pure sliding, the peeling force asymptotes to a maximum finite value. As will be demonstrated in the next section, the vertical component of the critical force in one side of the 'V'-peel test (Fig. 3A) is identical to the vertical component of the critical force in the single sided peel test (Fig. 3B).

It is worth emphasizing that Eqs. (18–23) reference the *deformed* peel angle, as opposed to the initial peel angle at the start of a test. Experiments that monitor the load and the deformed peel angle can be used to immediately calculate the work of adhesion via Eqs. (18–23), assuming strains are small. The evolution of peel length (or angle) under monotonically increasing force, starting from an initially unloaded "V" configuration is discussed in Section 5.3.

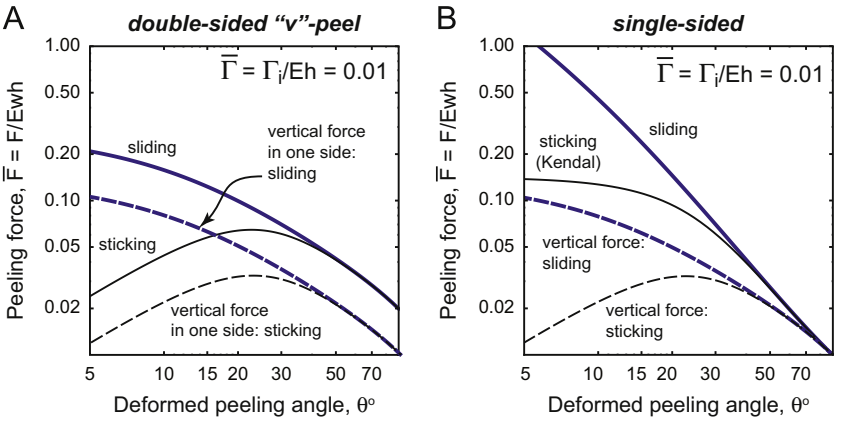

Fig. 3. Critical force to propagate peeling as a function of deformed peeling angle, for (A) double-sided "V" peeling and (B) single-sided peeling. Results are shown for both the present sliding analyses, as well the Kendall-type pure sticking analyses. The results are shown on the same scale to highlight the fact that "V" peeling requires much smaller forces than single sided peeling: however, the vertical component of the force in one side is equal to the vertical component of the force in the single-sided peel test.

4. Single-sided peeling

4.1. General analysis

The analysis of single-sided peeling follows the same procedure as above, with several simple modifications. First, the change in deformed angle θ associated with a peeling increment dL_0 is zero because the tape must remain oriented in the direction of the applied force. Hence, the incremental displacements (dx_D, dy_D) of the load-point are given by Eqs. (5) and (6) with $d\theta = 0$. This implies the work increment associated with the increment in load point displacement is given by

$$dW_F = F\cos\theta \cdot dx_D + F\sin\theta \cdot dy_D = F(\lambda_D\, dL_0 + L_0\, d\lambda_D) + F\cos\theta\left(\frac{df}{d\lambda}d\lambda_A - dL_0\right) \tag{24}$$

The analysis of the work done at the edge of attachment is identical, except the tape tension component in the x-direction at point A is given by $F\cos\theta$ instead of $F/(2\tan\theta)$, so that

$$dW_A = F\cos\theta\left(\frac{df}{d\lambda}d\lambda_A - (\lambda_A - 1)\, dL_0\right) \tag{25}$$

With similar substitution of the proper tape tension, the change in strain energy becomes

$$dU_D = wh\psi(\lambda_D)\, dL_0 + FL_0\, d\lambda_D \tag{26}$$

Putting it all together as before (but recognizing there is now only one tape leg and attachment point), one obtains

$$Gw\, dL_0 = F(\lambda_D\, dL_0 + L\, d\lambda_D) + F\cos\theta\left(\frac{df(\lambda_A)}{d\lambda}d\lambda_A - dL_0\right) - wh\psi(\lambda_D)\, dL_0 - FL_0\lambda_D + wh\psi(\lambda_A)\, dL_0 - F\cos\theta\left(\frac{df(\lambda_A)}{d\lambda}d\lambda_A + (\lambda_A - 1)\, dL_0\right) \tag{27}$$

where G is the energy released by peeling. Eq. (18) simplifies to

$$G = \frac{F}{w}(\lambda_D - \lambda_A\cos\theta) + h(\psi(\lambda_A) - \psi(\lambda_D)) \tag{28}$$

Once again, this expression is a universal result valid for the single-sided peeling of any elastic material, as long as the frictional drag is consistent with our assumptions. For pure sticking, $\lambda_A = 1$ and $\psi(\lambda_A) = 0$, and we recover Kendall's (1971, 1975) classic result. Finally, we note that this result is identical to that of double-sided peeling, provided one defines the effective force as the component aligned with the tape: i.e., if one replaces F in Eq. (28) with $F/(2\sin\theta)$ (the tape tension for double-sided V-peeling), one recovers Eq. (18).

4.2. Energy released by peeling for small strains: single-sided peeling

For single-sided peeling, we have

$$\epsilon_D = \frac{F}{Ehw}, \quad \epsilon_A = \frac{F\cos\theta}{Ewh}, \quad \psi(\lambda_D) = \frac{E}{2}\left(\frac{F}{Ewh}\right)^2, \quad \psi(\lambda_A) = \frac{E}{2}\left(\frac{F\cos\theta}{Ewh}\right)^2 \tag{29}$$

As before, the convenient normalized variables are $\overline{F} = F/(Ewh)$ and $\overline{G} = G/(Eh)$. With these results, Eq. (28) becomes

$$\overline{G} = \overline{F}(1 - \cos\theta) + \frac{1}{2}\overline{F}^2\sin^2\theta \tag{30}$$

Inverting, the critical force necessary to sustain peeling is given by

$$\overline{F}_c = \frac{1}{\sin\theta}\left(\sqrt{2\overline{\Gamma} + \tan^2\frac{\theta}{2}} - \tan\frac{\theta}{2}\right) \tag{31}$$

Again, this result is no longer universal as it cannot be used for pure sticking. Also, it represents the steady-state result, since θ and $\overline{F}$ do not change as the displacement of the unattached end increases. That is, single-sided peeling is by definition at steady-state assuming the direction of the loading is fixed.

To obtain the pure sticking result for infinitesimal strain first developed by Kendall (1975), we set $\epsilon_A = 0$ and $\psi(\lambda_A) = 0$ and deduce from Eq. (28) the following:

$$\overline{G} = \overline{F}(1 - \cos\theta) + \frac{1}{2}\overline{F}^2 \tag{32}$$

Solving for the peel force required to propagate peeling, we get Kendall's (1975) result for a non-sliding tape:

$$\overline{F}_K = \left(\sqrt{2\overline{\Gamma} + 4\sin^4\frac{\theta}{2}} - 2\sin^2\frac{\theta}{2}\right) \tag{33}$$

where $\overline{F}_K = F_K/(Ewh)$ denotes the (dimensionless) critical force predicted by Kendall (1975) for pure sticking.

Fig. 3B illustrates the dimensionless critical forces (required to propagate peeling) for sliding and pure sticking, as a function of peel angle, for infinitesimal strains. Note that as $\theta \to 0$, the sliding case predicts $F \to \infty$, in contrast to the outcome of the pure sticking case, where $F_K \to w\sqrt{2\Gamma_i E h}$. The peeling angle at which the two predictions (sliding and pure sticking) diverge is a function of $\overline{\Gamma}_i$: as the interface adhesion energy increases, the divergence occurs at larger and larger angles. For $\overline{\Gamma}_i \ll 1$, the predictions agree at most practical angles except for θ less than a few degrees: this is simply because $\overline{F}$ will scale with $\overline{\Gamma}_i$, such that small $\overline{\Gamma}_i$ implies $\overline{F}^2 \ll \overline{F}$.

Also, it is worth noting that the vertical component of the critical force during peeling with sliding but involving infinitesimal strain is given by

$$\overline{F}_y = \overline{F}\sin\theta = \sqrt{2\overline{\Gamma} + \tan^2\frac{\theta}{2}} - \tan\frac{\theta}{2} \tag{34}$$

which remains finite as $\theta \to 0$ despite the divergence of the total peel force required to propagate peeling. This result is also plotted in Fig. 3B for infinitesimal strains, along with the corresponding result from the pure sticking solution. The vertical component of the force in the single sided peel test is identical to the vertical component of the force in one side of the double-sided 'V' -peel test. That is, Eq. (34) is exactly one-half of Eq. (21) for the double-sided peel test.

5. Discussion

5.1. Work contributions for single-sided peeling

Peeling with sliding enhances the effective toughness of the tape adhesion when the peel angle is very low, but does not enhance the adhesion, in the sense that the force orthogonal to the substrate needed to overcome adhesion is not increased beyond the level dictated by the local adhesion energy. In contrast, in the pure sticking case (Kendall's, 1975 solution), the normal force actually decreases with peel angle for small peel angles (see Fig. 3B). This is an important difference: in the present approach, as the peel angle approaches zero, the tape merely slides.

The work done on the attached tape during detachment by single-sided peeling is given by Eq. (25). In the case of infinitesimal strain and a given peel angle, the force required to propagate peeling remains fixed while the tape detaches, and thus $d\lambda_A = 0$ during peeling. It follows then that the work computed from Eq. (25) is entirely dissipated via friction. In this case, the work dissipated by friction is given by

$$\frac{1}{Ewh}\frac{\delta W_A}{\delta L} = (\overline{F}\cos\theta)^2 \tag{35}$$

where δ has been used in the infinitesimal ratio in Eq. (35) because it is dissipated work and not a reversibly stored quantity. The ratio of frictional work dissipated to the energy released to adhesion is then

$$\frac{1}{\Gamma w}\frac{\delta W_A}{\delta L} = \frac{\overline{F}\cos^2\theta}{1-\cos\theta+\frac{1}{2}\overline{F}^2\sin^2\theta} \tag{36}$$

Since Eq. (31) indicates that $\overline{F} \to \sqrt{2\overline{\Gamma}}/\theta$ when $\theta \to 0$, it is straightforward to show that the ratio of frictional work to energy released then goes to infinity in Eq. (36). Thus, as $\theta \to 0$, the work of the applied load increasingly goes into frictional sliding and little is left over to drive detachment.

When $\theta = \pi/2$, such that the tape is being pulled vertically from the substrate, the critical force required to drive peeling with infinitesimal strain predicted for sliding and pure sticking coincide: this reflects the fact that no sliding occurs in this case. (Some trigonometric manipulation of Eqs. (31) and (33) is required to establish this point). When the peel angle is greater than $\pi/2$, the attached segment of the sliding tape will be in compression, leading to the possibility that it may buckle as it slides, thus detaching in a complicated mechanism. However, if the peel phenomenon remains consistent with our analysis (i.e., without buckling or wrinkling or other deviations from simple sliding), the force required during sliding with infinitesimal strain will differ from that predicted by Kendall's (1975) model, given that adhesion energy is the same in both cases. However, the limit of Eq. (31) when $\theta \to \pi$ is $F = \Gamma w/2$, which can be confirmed by inspection of Eq. (33) in the same limit. Interestingly, Kendall's result (Eq. (33)) provides the same force in this limit, after the fact that $\overline{F} \ll 1$ has been taken into account.

The limiting result from Eq. (31) as $\theta \to \pi$ is straightforward to understand. The strain energy in the attached tape that is peeled off is exactly the same as that in the detached tape when $\theta = \pi$, so the work to compensate for the adhesion energy (as the tape detaches) is provided entirely by the applied load. The free end of the unattached tape is moving at twice the rate at which the tape detaches, plus an amount proportional to the strain in the detached tape times the rate of detachment of the tape. However, as indicated by Eq. (24), the rate of work required by frictional sliding when $\theta \to \pi$ is equal to the applied load times the strain in the attached tape times the rate of detachment of the tape. Therefore, the work not absorbed by friction is twice the applied load times the incremental length of tape that is peeled off. This work has to equal the adhesion energy, $\Gamma w dL$, leading to a peeling force equal to $\Gamma w/2$, as noted above.

As indicated above, when $\theta \to \pi$, the sliding absorbs work, equal to the applied load times the strain in the attached tape times the incremental length of tape being peeled off. This amount of work is given by Eq. (25), so that, in the case of $\theta = \pi$,

this work is equal to $\Gamma^2 wdL/(4Eh)$, indicating that there is a sliding displacement during detachment equal to $\Gamma dL/(2Eh)$, in agreement with Eq. (3). The ratio of work absorbed by friction to that absorbed by the adhesion energy is thus $\Gamma/(4Eh)$ when the strains are infinitesimal, while the total effective toughness at $\theta=\pi$ is $\Gamma(1+\Gamma/(4Eh))$, being the sum of the adhesion energy and the work dissipated in friction.

5.2. Mixed-mode fracture analog for single-sided peel test

The debonding of thin films from substrates has been intensively studied using mixed-mode fracture mechanics, which predicts detachment when the energy released by debonding reaches a critical value for the interface, referred to as the interface toughness (Thouless and Yang, 2008; Sun and Dillard, 2010). The impact of dissipation mechanisms (e.g., frictional sliding and/or plastic deformation) that occur close to the crack tip is accounted for by defining a "mixed-mode" interface toughness: i.e., $G_c(\phi)$, where the phase angle is defined by the ratio of shear (sliding) and normal (opening) stresses ahead of the crack, i.e., $\tan\phi=\lim_{r\to 0}[\sigma_{xy}/\sigma_{yy}]$. This approach is distinctly different from the methodology adopted above: dissipation near the crack tip is not resolved explicitly and factored into the calculation of forces (as we do above), but rather lumped into the energy that must be supplied to the edge of detachment to drive debonding (Newby and Chaudhury, 1997; Thouless and Yang, 2008). The key point to emphasize is that the mixed-mode fracture toughness $G_c(\phi)$ is *not* equivalent to the adhesion energy (Γ_i) in the above discussion, but rather is equal to the adhesion energy plus any frictional work that must be supplied to drive detachment. In that sense, the sliding case analyzed by us in the present paper is effectively experiencing a dramatic increase in the *interface toughness*, since the work dissipated against friction is unavoidable while detachment is taking place.

Rather than explicitly incorporating the frictional work into the analysis as done above, one could take an alternative approach, wherein the pure sticking (Kendall) result is used with a mixed-mode interface toughness $G_c(\phi)$, which incorporates the effects of frictional sliding. The membrane analysis used here precludes a rigorous definition of a phase angle, which strictly speaking requires resolution of the bending fields at the edge of the attachment (Thouless and Yang, 2008). Nevertheless, a reasonable approach is to define the phase angle by $\tan\phi=F_x/F_y$, where F_x and F_y are the force resultants at the edge of the attachment zone. This implies $\phi=\pi/2-\theta$, with the usual interpretation that $\phi=0$ ($\theta=\pi/2$) is pure mode I behavior, and $\phi=\pi/2$ ($\theta=0$) is pure mode II behavior.

We define an effective mixed-mode interface toughness $G_c(\phi)$ as follows: we equate the two critical forces needed for peeling obtained by setting the energy released by peeling for pure sticking to $G_{stick}=G_c(\phi)$ and the energy released by peeling with sliding to $G_{slide}=\Gamma_i$. Solving for $G_c(\phi)=f(\Gamma_i,\phi)$ yields the mixed-mode interface toughness that should be used with the pure sticking (Kendall) result to account for frictional sliding by lumping dissipated work into the interface toughness. Put another way, using the pure sticking result with $G_c(\phi,\Gamma_i)$ leads to the same critical peeling force as a sliding analysis.

The result of this exercise, for infinitesimal strain, is

$$\frac{G_c}{\Gamma_i}=f(\phi,\overline{\Gamma}_i)=[1+(1-\alpha(\phi,\overline{\Gamma}_i))\tan^2\phi]$$

$$\alpha(\phi,\overline{\Gamma}_i)=\frac{\sqrt{6+4\overline{\Gamma}_i+(4\overline{\Gamma}_i-2)\cos 2\phi-8\sin\phi+4\overline{\Gamma}_i+6}+2\sin\phi-2}{2\overline{\Gamma}_i(1+\sin\phi)} \tag{37}$$

where $\overline{\Gamma}_i=\Gamma_i/(Eh)$, as before, and ϕ, when peeling involves infinitesimal strain, represents the mode-mixity phase angle. Plots of the apparent interface toughness versus mode-mixity are shown in Fig. 4 for two values of the normalized adhesion energy $\overline{\Gamma}=\Gamma/(Eh)$. Two limits are immediately obvious: for pure mode I, $\phi=0$ ($\theta=\pi/2$), and the effective interface toughness (G_c) asymptotes to the adhesion energy (Γ_i). For pure mode II, $\phi=\pi/2$ ($\theta=0$), the interface toughness asymptotes to infinity, a consequence of the increased role of frictional dissipation that must be overcome to drive detachment.

Interestingly for the present peeling problem, the impact of mode-mixity on the apparent interface toughness is a function of the adhesion energy itself: large values of $\overline{\Gamma}$ lead to stronger mode-mixity effects. Physically, this is a consequence of the fact that large adhesion energies will require larger forces to drive peeling, which in turn will increase the length of the shear sliding zone and thus increase the amount of frictional work that must be overcome to drive detachment.

The form of Eq. (37) allows for direct comparisons to other mixed-mode thin film fracture studies (Evans et al., 1990; Hutchinson and Suo, 1992), which adopt the same form with α taken as a constant: in previous approaches, α is an empirical fitting constant determined from mixed-mode fracture data. Results of this approximation are plotted in Fig. 4 for $\alpha=0.15$ and 0.92, and show excellent agreement with the full sliding model; that is, $\alpha=0.15$ is the empirical fitting constant that works for large adhesion energies ($\overline{\Gamma}_i=1$) and $\alpha=0.92$ is the empirical fitting constant that works for small adhesion energies ($\overline{\Gamma}_i=0.001$). It should be noted that this quasi-empirical approach is absolutely necessary if the dissipative mechanisms near the crack tip are not explicitly modeled as we have done above (with friction in the present paper), since one cannot easily experimentally separate the effects of adhesion and dissipative mechanisms such as friction.

Once again, it is perhaps surprising that the shear sliding stress does not factor into the apparent mixed-mode interface toughness, given that the increase in apparent toughness arises due to frictional work dissipated when mode II effects are significant (i.e., at low peeling angles). However, the relative contributions of frictional sliding and the normal work of separation are implicitly accounted for through the strength of the adhesion: large adhesion energies lead to large sliding

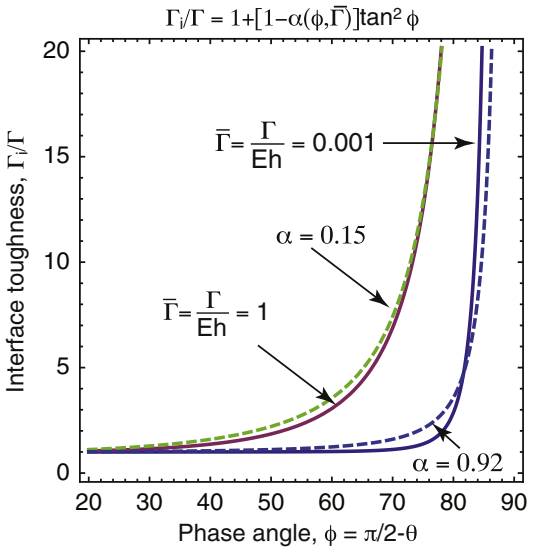

Fig. 4. Inferred mixed-mode interface toughness as a function of phase angle (peel angle) that needs to be used with a pure sticking model to predict the same critical force to drive peeling as the current frictional sliding model. The impact of mode-mixity on the inferred toughness increases with adhesion energy, due to increased frictional dissipation in the sliding zone. Also shown are predictions with α constant, which is a common form inferred from mixed-mode fracture experiments.

zones, which increase the apparent toughness, as shown in Fig. 4. For small adhesion energies, normal separation occurs prior to significant sliding, such that sliding effects on the apparent toughness are only pronounced for scenarios with dominant mode II components: i.e., large phase angles which correspond to small peeling angles.

It is worth noting that the mode-dependence of interface toughness due to plastic deformation has been modeled, with the interface toughness predicted as a function of adhesion energy and the elastic–plastic properties of the film (Wei and Hutchinson, 1998); this exercise leads to plots that are extremely similar to those shown in Fig. 4, with the strength of mode-mixity governed by a dimensionless parameter involving the adhesion energy and yield strength of the film. In a sense, Eq. (37) is an analogous theoretical result that captures frictional sliding effects (rather than yielding effects).

5.3. *Peeling propagation for double-sided peeling with constant frictional shear stress*

Here, we consider the evolution of the deformed peel angle as a function of applied force, which is necessary to calculate load–displacement curves for the peel test. Reference is made to the unstressed but peeled state (shown in Fig. 1C): the unstressed detached length L_0 and the unstressed angle θ_0 can be considered as implicit parameters that define the current detached length during loading: these are eventually eliminated in favor of results cast purely in terms of the initial and deformed configurations, which are experimentally observable.

We will consider only the case of a uniform sliding stress τ, i.e., one that does not depend on sliding displacements. The displacements in the sliding region can be determined via a shear-lag analysis involving infinitesimal strain, with the boundary conditions that displacements are zero at X_A and the force in the tape at the edge of detachment in the deformed condition is $F/(2\tan\theta)$. This analysis yields

$$x_A = X_A - \frac{F^2}{8E\tau w^2 h\tan^2\theta} = L_0\cos\theta_0 - \frac{F^2}{8E\tau w^2 h\tan^2\theta} \tag{38}$$

where x_A represents the position of the edge of detachment, i.e., the debond length. The length of one detached branch, AD, in the loaded configuration is given by

$$L_0\left[1+\frac{F}{2Ewh\sin\theta}\right] = \frac{x_A}{\cos\theta} \tag{39}$$

We eliminate x_A between Eq. (38) and Eq. (39) to obtain

$$\frac{F^2}{8E\tau w^2 hL_0\tan^2\theta} + \frac{F}{2Ewh\tan\theta} + \cos\theta - \cos\theta_0 = 0 \tag{40}$$

The relevant root of this equation is

$$\bar{F} = 2\hat{\tau}\bar{L}_0\left[\sqrt{1+\frac{2[\cos\theta_0-\cos\theta]}{\hat{\tau}\bar{L}_0}}-1\right]\tan\theta \tag{41}$$

where $\overline{F}=F/(Ewh)$ as before, $\overline{L}_0=L_0/h$, and $\hat{\tau}=\tau/E$. Note that there is nothing that is automatically infinitesimal in Eq. (41), though the result must be consistent with $\overline{F}\ll 1$, placing a restriction on its range of validity as θ is increased.

For the initiation of peeling from an unstressed "V" configuration, $\theta_0=\theta_i$ and $L_0=L_i$; the deformed configuration and critical force can be found by simultaneous solution of $\overline{G}=\overline{\Gamma}_i$, Eq. (39) and Eq. (41), where x_A, $\overline{F}$ and θ are the unknowns. This assumes, of course, that the shear sliding stress is known. On the other hand, if the deformed angle θ and force at the initiation of peeling are measured, one can directly compute the shear sliding stress; in this case, the debond length x_A provides a second measure of the validity of the underlying assumptions, since Eq. (38) holds.

After the propagation of peeling, the unstressed state (defined by L_0 and θ_0) for the current peeled configuration is no longer known, due to the fact that each peeling increment occurs from a different unstressed peeled length. To extract the behavior during propagation of peeling, one can specify θ_0 as an implicit parameter that defines the current peeled length, and solve for the deformed geometry as a function of peeled force. To do so, L_0 must be cast in terms of θ_0 and the initial configuration, L_i and θ_i.

Referring to Fig. 1, we denote the distance from the edge of detachment in the initial state to the end of the tape as s_i; similarly, the distance from the edge of detachment in the unstressed reference state to the end of the tape is denoted as s_0. Since both the initial state and reference state are unstressed, the length of the tape from the tip of the "V" to its end must be the same in both configurations, hence: $L_i+s_i=L_0+s_0$. The distance along the substrate, from the centerline to the end of the tape, must also be equal: $L_i\cos\theta_i+s_i=L_0\cos\theta_0+s_0$. Eliminating s_i and s_0 from these equations yields

$$L_0=\left(\frac{1-\cos\theta_i}{1-\cos\theta_0}\right)L_i \tag{42}$$

Substituting this result into Eq. (41), one obtains

$$\overline{F}=2\overline{\tau}\left(\sqrt{1+\frac{2(1-\cos\theta_0)(\cos\theta_0-\cos\theta)}{\overline{\tau}(1-\cos\theta_i)}}-1\right)\left[\frac{(1-\cos\theta_i)\tan\theta}{1-\cos\theta_0}\right] \tag{43}$$

where the normalized shear stress becomes

$$\overline{\tau}=\frac{\tau L_i}{Eh} \tag{44}$$

For a given initial configuration defined by θ_i and a given peeled length defined implicitly by θ_0, one then solves Eq. (21) and Eq. (43) to find $\overline{F}$ and θ, the parameters defining the deformed state. The debonded length (i.e., the distance to the edge of attachment) can be computed by combining Eq. (39) with Eq. (42):

$$x_A=L_i\cos\theta\left(\frac{1-\cos\theta_i}{1-\cos\theta_0}\right)\left(1+\frac{\overline{F}}{2\sin\theta}\right) \tag{45}$$

Regarding experimental parameter extraction, if the deformed state of the tape is known (i.e., $\overline{F}$, θ and x_A), one can compute θ_0 from Eq. (45), and compute work of adhesion from Eq. (21) and the effective shear sliding stress from Eq. (43).

In Fig. 5A, we illustrate the results for the critical force to initiate peeling when strains are infinitesimal as a function of the angle of the initial unstressed geometry. The critical force to start peeling is a function of the shear sliding stress because sliding permits the edge of the tape to slide inwards prior to any peeling: this sliding re-orients the angle of

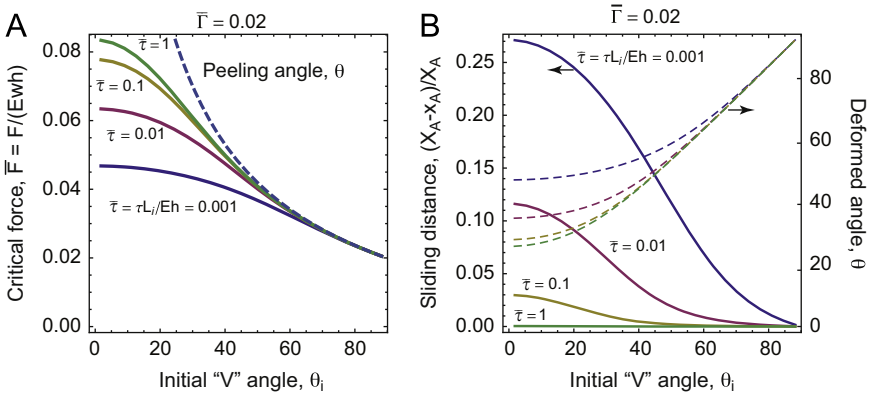

Fig. 5. (A) Critical force to drive peeling at the onset of peeling versus initial (unloaded angle) and (B) the sliding distance (i.e., change in debond size) at the onset of peeling as a function of initial angle, for several different values of the normalized sliding stress, $\overline{\tau}=\tau L_i/(Eh)$. The dashed line indicates the deformed angle: the deformed angle is larger than the initial (unloaded angle) because of elastic stretching in the tape and inward sliding of the detachment point. Friction influences the initial geometry associated with a given critical force, but not the angle in the deformed state at the onset of peeling.

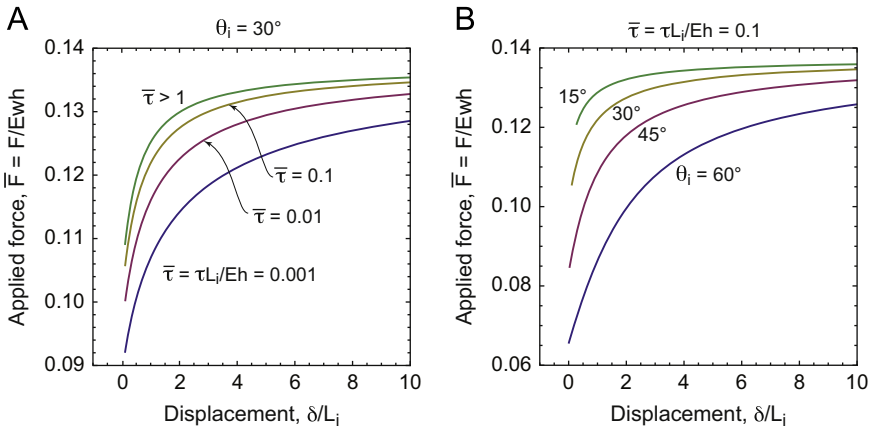

Fig. 6. Force displacement curves for several different sets of parameters for peeling propagation. Decreasing the frictional sliding stress increases the load point displacement but does not influence the force for a given peeling angle (referenced to the deformed state). Increasing the frictional sliding stress decreases the displacement at which steady-state peeling is reached, wherein a constant force coincides with a constant peel angle (referenced to the deformed state).

attachment, increasing the vertical force component at the edge of attachment and lowering the critical force needed for peeling. The amount of sliding is illustrated in Fig. 5B, which illustrates the change in the detached length along the surface at the instant of peeling when strains are infinitesimal: as the sliding stress decreases, inward sliding increases: inward sliding decreases with initial angle due to the decrease in tangential force at the edge of attachment. Note that the critical force is independent of the sliding stress when expressed as a function of the deformed angle (as opposed to the initial angle), as shown by the dashed line. The dashed curves in Fig. 5B illustrate that the change in angle between the initial unstressed geometry and the deformed geometry at the instant of peeling initiation decreases with increasing sliding stress.

It is worth emphasizing that for $\theta_i = 0$, we assume that there is still a central region of length $2L_i$ in which there are no adhesive forces between the tape and substrate, despite the fact that the tape is lying flat. From the edge of this "no adhesion zone" outwards, the tape remains adhered with work of separation defined as Γ_i. As mentioned above, an analysis of a perfectly flat tape with adhesive forces everywhere requires explicit reference to the cohesive law describing the surface interactions: this case will be treated in future papers.

For normalized shear stresses $\overline{\tau} > \approx 1$, the critical force and change in angle due to loading is effectively independent of the sliding stress parameter, because sliding displacements become negligible. Even so, in the limit of no sliding the current predictions still predict peeling angles that are much larger than the initial angle: this is because the driving force for detachment is the vertical component of the tape tension, such that the deformed angle must be increased until this component reaches a critical value. Thus, in the limit of zero sliding, our results become independent of sliding stress but are still very different than models that assume that horizontal force components will drive detachment, i.e., the results in Kendall (1975). For this reason, the critical forces shown in Fig. 5A for high sliding stresses are still higher than Kendall-type models (even with no sliding) because the present models assume that horizontal forces do not play a role in detachment.

Fig. 6 illustrates force–displacement curves for 'V'-peeling for several values of the shear sliding stress and several initial angles when strains are infinitesimal. After initiation, the force required to drive detachment increases because peeling extends the undeformed length of tape, effectively lowering the "initial angle" corresponding to an unstressed geometry. The curves all asymptote to the same peak load, which corresponds to the scenario where the angle of the unstressed, peeled geometry is equivalent to the critical value of the deformed angle. As the sliding stress decreases, the applied displacement required to reach steady-state peeling increases, again due to inward sliding which re-orients the tape in the deformed configuration. Once again, the results in Fig. 6A become independent of sliding stress for $\overline{\tau} > \approx 1$, such that the top curve represents the results in the limit of no sliding. Again, even though no sliding is present, the curves are very different than Kendall-type models because of the critical role of normal forces (as opposed to tape tension): as the tape peels, the undeformed angle is changed, changing the force needed to reach the critical normal force at the edge of detachment. Fig. 6B illustrates the fact that the displacement required to reach steady-state decreases with decreasing initial angle for infinitesimal strains: this is because in the limit of zero initial angle, the length of initially detached tape does not influence the normal force at the edge of attachment in the deformed state.

Finally, Fig. 7 illustrates the peeling angle (i.e., the angle in the deformed state) as a function of applied displacement when strains are infinitesimal. The evolution of tape geometry during peeling is also shown in the lines above the plots, which are to-scale. As the tape is pulled upwards, the peeling angle decreases from an initially high value to the lower steady-state value. For low sliding stress, inward sliding can considerably increase the angle at the initiation of peeling from its initial undeformed value to that prevailing. Again, low peel angles show the most "brittle" behavior, in that smaller displacements are required to reach the steady-state peel angle.

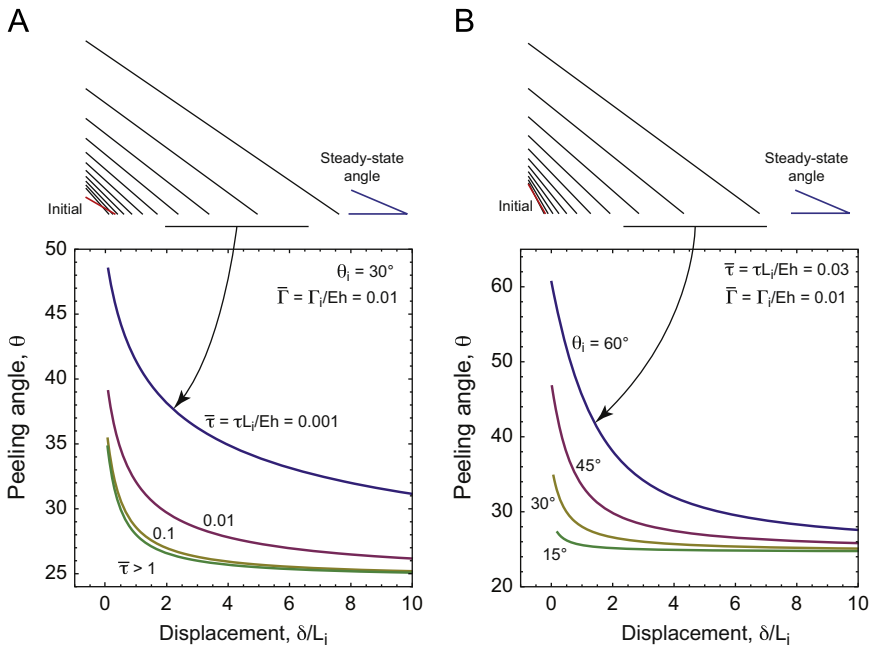

Fig. 7. Peel angle (deformed, under load) as a function of applied displacement for several values of shear sliding stress (A) and several initial (undeformed) angles (B): for $\bar{\tau} \geq 1$, the results are independent of shear sliding stress. The deformed profiles corresponding to the top curves are shown above the framed figures: the red line indicates the initial undeformed shape. (For interpretation of the references to color in this figure legend, the reader is referred to the web version of this article.)

6. Conclusions

The assumption that arbitrary sliding displacements can occur without peeling in membrane tapes leads to the existence of elegant closed-form results for the energy released by peeling that do not depend on the nature of the shear stress that resists sliding; critical peel forces are controlled purely by the vertical component of the adhesion force at the edge of attachment. The dissipated work done in frictional sliding during peeling is accommodated and inherently balanced by an increase in the work done by the applied load. For single-sided peeling, where the peel angle does not change, peeling propagates at steady-state when the critical load is reached: regardless of their nature, the shear sliding stress and the resulting sliding displacements have no bearing on the critical force for peel propagation. Furthermore, the analysis which allows for sliding leads to very different predictions than the conventional one based on pure sticking. This is because the conventional analysis for pure sticking assumes that force applied to the tape tangential to the substrate at the edge of attachment can drive peeling, in addition to the effect of forces normal to the substrate. In the present analysis, the forces applied to the tape tangential to the substrate do not contribute to the energy released by peeling: rather, they cause sliding that is accommodated by additional motion of the load point, and only forces normal to the substrate drive detachment.

In double-sided peeling, where tangential sliding and the deformed peeling angle are coupled, frictional sliding alters the displacement required to reach steady-state, implying that increasing forces are required to drive peeling. After sufficient peeling, the force asymptotes to a steady-state value. Above a critical shear sliding stress, $\tau L_i/Eh > \approx 1$, the force–displacement curves are independent of shear sliding stress. Again, the predicted critical forces for peeling propagation are very different than those obtained from the conventional pure sticking analysis, owing to the fact that the components of detached tape tension parallel to the substrate at the edge of detachment do not factor into the energy released by detachment. By equating the critical forces obtained from sliding and pure sticking analyses, one can define an effective macroscopic mixed-mode fracture toughness for both single sided and 'V'-peeling, that depends on the adhesion energy for normal separation and the peel angle.

Acknowledgments

M.R.B. and R.R.C. gratefully acknowledge the support of the National Science Foundation through CMII Grant no. #1063714 (formerly #0800790). M.R.B., R.R.C. and J.N.I. also gratefully acknowledge the support of the National Science Foundation through MRSEC Program DMR-1121053 (MRL-UCSB). Partial support was also provided for M.R.B., R.R.C. and J.N.I. by the Institute for Collaborative Biotechnologies through Contract no. W911NF-09-D-0001 from the U.S. Army Research Office. The content of the information does not necessarily reflect the position or the policy of the Government, and no official endorsement should be inferred.

References

Amouroux, N., Petit, J., Leger, L., 2001. Role of interfacial resistance to shear stress on adhesive peel strength. Langmuir 17, 6510–6517.

Chen, B., Wu, P.D., Gao, H.J., 2009. Pre-tension generates strongly reversible adhesion of a spatula pad on substrate. J. R. Soc. Interface 6, 529–537.

Cheng, Q.H., Chen, B., Gao, H.J., Zhang, Y.W., 2012. Sliding-induced non-uniform pre-tension governs robust and reversible adhesion: a revisit of adhesion mechanism of geckos, J. R. Soc. Interface 9, 283–291.

Evans, A.G., Rühle, M., Dalgleish, B.J., Charalambides, P.G., 1990. The fracture energy of bimaterial interfaces. Mater. Sci. Eng. A 126, 53–64.

Gent, A.N., Kaang, S., 1986. Pull-off forces for adhesive tapes. J. Appl. Polym. Sci. 32, 4689–4700.

Hutchinson, J.W., Suo, Z., 1992. Mixed mode cracking in layered materials. Adv. Appl. Mech. 29, 63–191.

Kendall, K., 1971. The adhesion and surface energy of elastic solids. J. Phys. D: Appl. Phys. 4, 1186–1195.

Kendall, K., 1975. Thin-film peeling—the elastic term. J. Phys. D: Appl. Phys. 8, 1449–1452.

Kinloch, A.J., Lau, C.C., Williams, J.G., 1994. The peeling of flexible laminates. Int. J. Fract. 66, 45–70.

Lu, Z.X., Yu, S.W., Wang, X.Y., Feng, X.Q., 2007. Effect of interfacial slippage in peel test: theoretical model. Eur. Phys. J. E 23, 67–76.

Molinari, A., Ravichandran, G., 2008. Peeling of elastic tapes: effects of large deformations, pre-straining, and of a peel-zone model. J. Adhes. 84, 961–995.

Newby, B.-M.Z., Chaudhury, M.K., 1997. Effect of interfacial slippage on viscoelastic adhesion. Langmuir 13, 1805–1809.

Newby, B.-M.Z., Chaudhury, M.K., 1998. Friction in adhesion. Langmuir 14, 4865–4872.

Newby, B.-M.Z., Chaudhury, M.K., Brown, H.R., 1995. Macroscopic evidence of the effect of interfacial slippage on adhesion. Science 269, 1407–1409.

Pesika, N.S., Tian, Y., Zhao, B., Rosenberg, K., Zeng, H., McGuiggan, P., Autumn, K., Israelachvili, J.N., 2007. Peel-zone model of tape peeling based on the gecko adhesive system. J. Adhes. 83, 383–401.

Plaut, R.H., Ritchie, J.L., 2004. Analytical solutions for peeling using beam-on-foundation model and cohesive zone. J. Adhes. 80, 313–331.

Sauer, R.A., 2011. The peeling behavior of thin films with finite bending stiffness and the implications on gecko adhesion. J. Adhes. 87, 624–643.

Sun, Z., Dillard, D.A., 2010. Three-dimensional finite element analysis of fracture modes for the pull-off test of a thin film from a stiff substrate. Thin Solid Films 518, 3837–3843.

Sun, Z., Wan, K.-T., Dillard, D.A., 2004. A theoretical and numerical study of thin film delamination using the pull-off test. Int. J. Solids Struct. 41, 717–730.

Thouless, M.D., Yang, Q.D., 2008. A parametric study of the peel test. Int. J. Adhes. Adhes. 28, 176–184.

Tsai, K.-H., Kim, K.-S., 1993. Stick-slip in the thin film peel test-I. the 90° peel test. Int. J. Solids Struct. 30, 1789–1806.

Tvergaard, V., Hutchinson, J.W., 1993. The influence of plasticity on mixed mode interface toughness. J. Mech. Phys. Solids 41, 1119–1135.

Wan, K.-T., 1999. Fracture mechanics of a V-peel adhesion test—transition from a bending plate to a stretching membrane. J. Adhes. 70, 197–207.

Wang, S.J., Li, X., 2007. The effects of tensile residual stress and sliding boundary on measuring the adhesion work of membrane by pull-off test. Thin Solid Films 515, 7227–7231.

Wei, Y., Hutchinson, J.W., 1998. Interface strength, work of adhesion and plasticity in the peel test. Int. J. Fract. 93, 315–333.

Williams, J.G., 1997. Energy release rates for the peeling of flexible membranes and the analysis of blister tests. Int. J. Fract. 87, 265–288.